ISSN 0915-633X

NATIONAL INSTITUTE FOR FUSION SCIENCE

Measurement of Internal Magnetic Field with Motional Stark Polarimetry in Current Ramp-Up Experiments of JIPP T-IIU

J. Xu, K. Toi, H. Kuramoto, A. Nishizawa, J. Fujita, A. Ejiri,
K. Narihara, T. Seki, H. Sakakita, K. Kawahata, K. Ida, K. Adachi,
R. Akiyama, Y. Hamada, S. Hirokura, Y. Kawasumi, M. Kojima,
I. Nomura, S. Ohdachi, K.N. Sato

(Received - Apr. 25, 1996)

NIFS-419 June 1996

RESEARCH REPORT
NIFS Series

NAGOYA, JAPAN

Measurement of Internal Magnetic Field with Motional Stark Polarimetry in Current Ramp-Up Experiments of JIPP T-IIU

J. Xu, K. Toi, H. Kuramoto[1], A. Nishizawa, J. Fujita,
A. Ejiri, K. Narihara, T. Seki, H. Sakakita[2], K. Kawahata, K. Ida,
K. Adachi, R. Akiyama, Y. Hamada, S. Hirokura, Y. Kawasumi,
M. Kojima, I. Nomura, S. Ohdachi, K.N. Sato

National Institute for Fusion Science, Nagoya, 464-01, Japan
1) Kyusyu Inst. Tech., Iizuka 820, Japan
2) Nagoya University, Nagoya 464-01, Japan

Abstract

Multichannel polarization measurements of the Balmer α line of beam emission are performed using a 15-channel four-polarizer optical system on the JIPP T-IIU tokamak. The pitch angle of the internal magnetic field is obtained using a newly developed method where only σ-components of the motional stark spectrum are analyzed to avoid difficulty due to the π-component asymmetry caused by appreciable beam divergence. Radial profiles of internal poloidal magnetic field and safety factor are successfully obtained in a current ramp-up discharge. The safety factor at the magnetic axis q(0) is about 1.7 just before the current ramp-up and gradually decreases close to unity during the current ramping phase till the appearance of sawtooth oscillations. In the sawtoothing phase, q(0) is further decreased to be obviously below unity, i.e., 0.7-0.8, which suggests that no complete reconnection of the poloidal magnetic flux takes place at the sawtooth crash.

Keywords: Tokamak, Motional Stark Effect Polarimetry, Internal Poloidal Magnetic Field, Sawtooth, Partial Reconnection

§1. Introduction

Radial profile of the toroidal current density or the safety factor strongly affects the stability and confinement performance of a tokamak plasma. In an early stage of tokamak research, effectiveness of the current profile control on MHD stability had already demonstrated experimentally[1]. Later, the current density profile was controlled to induce the H-mode[2,3] and to produce high beta-poloidal plasmas[4]. Recently, in large tokamaks, the profile control is carried out to produce magnetic shear reversal in the plasma core region with various methods and to improve the plasma confinement [5, 6, 7, 8]. In these experiments, a direct measurement of the internal magnetic field is critically important to clarify the impact of the profile shape on plasma stability and plasma transport.

Several methods by means of Faraday rotation effect of launched laser beams or microwaves[9], Zeeman effect of visible lights[10, 11, 12], Alfvén wave resonance [13], and forward laser scattering[14] have been developed for the measurement in the past years. Recently, the motional Stark effect (MSE) of the Balmer α line emitted from a fast neutral hydrogen- or deuterium-beam (~50 keV/amu) injected into a toroidal plasma is recognized to be powerful to measure the local pitch angle of the internal magnetic field($\alpha_p=\tan^{-1}(B_p/B_t)$, B_p: poloidal magnetic field, B_t: toroidal magnetic field) and to obtain the safety factor profile with high accuracy. In the PBX-M and DIII-D tokamaks, the local pitch angle of the magnetic field is measured with a so-called polarimeter based on MSE [15, 16]. In the JET plasmas at the high toroidal magnetic field an optical system that in principle consists of a spectrometer and two polarizers tilted with respect to horizontal direction by $\pm 45°$ is applied to obtain the local pitch angle profile of the internal magnetic field[17].

Development of these powerful diagnostics for measurement of internal magnetic field profile also enables us to discuss whether or not a complete reconnection of poloidal magnetic flux takes place at the sawtooth crash and to compare the experimental results with existing theories on the sawtooth.

In this paper, we describe the MSE polarimetry carried out in a current ramp-up discharge of JIPP T-IIU. We have developed a four-polarizer optical system, and also developed a new analysis method of the MSE spectra which is based on using only σ components with the same optical system to derive the pitch angle. The MSE polarimetry has successfully carried out to measure the local pitch angle of the internal magnetic field in the current ramp up plasma. In Section 2, the four-polarizer optical system and the analyzing method of the measured spectra are described. In Section 3 we show the radial profiles of the safety factor obtained in the current ramp-up experiments. In Section 4 we discuss time evolution of the q-profile, in particular, of the q(0) in the current ramp-up plasma. We also discuss whether or not complete reconnection of the poloidal magnetic flux takes place at the sawtooth crash. Finally, we summarize our results in Section 5.

§2. Experimental Set-Up

2.1 MSE Polarimeter System

The JIPP T-IIU device is a medium sized tokamak with a major radius $R \approx 91$ cm and minor radius $a \approx 23$ cm, where the maximum toroidal magnetic field is 3 T [18]. Figure 1 shows the experimental arrangement of the MSE polarimeter system in JIPP T-IIU. A neutral hydrogen heating beam is injected into the plasma almost perpendicularly (9° tilted). In order to get Doppler shift of the beam emission line as large as possible, the port for the beam injection and that for the spectrum observation are separated toroidally by 66.4° as shown in Fig.1.

The optical system consists of four polarizers tilted by 0°, 45°, 90° and 135° with respect to the horizontal direction, respectively, which are put inside the vacuum chamber to avoid additional Faraday rotation when the light passes through a glass window of the port. The additional Faraday rotation is still induced by the polarizer itself, but it can be neglected because its thickness is very thin (~1 mm). Four lenses (focal length f=10 mm and diameter ϕ=10 mm) are arranged behind the polarizers and fifteen optical fibers with 0.1mm diameter are on the focal plane of the lens, viewing fifteen chords of the plasma. The spectroscopes are simultaneously recorded by an one-meter spectrometer equipped with a two dimensional (256pixel x256pixel) CCD detector with the intensity integration time of 20 ms. A 600 g/mm grating is used for our experiment. The wavelength dispersion of the spectrometer is carefully calibrated and wavelength resolution of the spectrometer is 1.8 Å in the interested wavelength region. The measurement region of the beam emission mainly covers a core plasma region of JIPP T-IIU from major radius R=83 cm to 109 cm. The spatial resolution of the measurement varies from 3 cm for the most inner chord to 6 cm for the most outer chord.

2.2 Pitch angle analysis

In the MSE polarimetry, the pitch angle is usually determined by analyzing the π component intensities of a diagnostic beam emission obtained from the signals of two polarizers. The MSE spectrum is fitted by a sum of Gaussians convoluted with the instrumental function of the spectrometer. It is comparatively easy to realize multichannel measurement of the pitch angle by applying this technique. However, since there is a spectral asymmetry in the π component as mentioned in reference [17], the spectrum fitting is expected to be difficult in practice due to many parameters. This difficulty is mainly caused by the large beam divergence which results in poor separation of each π component and large spectral asymmetry of the Stark feature. That is, it is more serious when a heating beam with fairly large divergence(> 1°) is used such as in our experiments. To overcome this difficulty, we have developed a new method where only σ-components are used to derive the local pitch angle of the magnetic field. In this subsection, we describe this spectral analysis method.

As is well known, the Balmer α line of hydrogen atom emission is split mainly into nine components due to the motional Stark effect[19], since there is the Lorentz electric field ($\mathbf{E}=\mathbf{V}_{beam} \times \mathbf{B}$) in the rest frame of the beam. The central σ component (Δm=1,-1) is polarized perpendicular to direction of the electric field, while the π components (Δm=0) distributed on both sides of the σ components have parallel polarization when they are observed transversely. Figure 2 shows a universal situation of the σ light transmission along the viewing line. The beam and the toroidal magnetic field are in the mid plane of the plasma, and the viewing line also lies on it. The Lorentz electric field is in a plane perpendicular to the mid plane. The straight line and circles stand for the linearly and circularily polarized parts of the σ components, respectively. The angle α_1 is the angle of the electric field with respect to the direction perpendicular to the mid plane, ψ the angle between the electric field and the viewing line, α the polarization angle of the σ line transmission along the viewing line, and β is the Doppler shift angle of the beam emission. The relations between the angles are

$$\tan\alpha = \tan\alpha_1 \cos\beta \qquad (1)$$

and

$$\cos\psi = \sin\alpha_1 \sin\beta. \qquad (2)$$

In an ideal case that the π manifolds are well separated from the σ manifold, the intensity of the σ emission is determined by each polarizer as

$$I_{1,2} = I_{\sigma c}/2 + I_{\sigma l}\cos^2(45 \pm \alpha). \qquad (3)$$

Here, $I_{\sigma c}$ and $I_{\sigma l}$ are the intensity of the circular and linear polarized part, respectively, in the σ component which satisfies a relation of $I_{\sigma c}/I_{\sigma l} = 2\cot^2\psi$. The relation between the angles and the measured intensities I_1 and I_2 can be obtained from equation (3) such that

$$\cot^2\psi = \frac{1}{2}\left(\frac{\xi+1}{\xi-1}\sin 2\alpha - 1\right). \qquad (4)$$

where, $\xi = I_2/I_1$. Taking account of the relation of the pitch angle α_p and the polarization angle α, $\tan\alpha_p = \tan\alpha \sin\zeta/\cos\beta$, the pitch angle can be expressed as

$$\tan\alpha_p = \sin\zeta\left\{\frac{\eta\cos\beta \pm \sqrt{\eta^2\cos^2\beta - (1+\sin^2\beta)}}{(1+\sin^2\beta)}\right\}, \qquad (5)$$

where ζ is the intersection angle of the beam with the magnetic field, and $\eta = (\xi+1)/(\xi-1)$. The '±' operation in the equation (5) is opposite to the sign of η.

§ 3. Experimental Results

The MSE polarimetry has been carried out in the current ramp-up experiment to test possibility of magnetic shear reversal, where the neutral beam of about 500 kW is injected into a torus for 120 ms. The hydrogen beam energy is 30 keV and the toroidal magnetic field is B_t=3.0 T at R=91 cm. Figure 3 shows time evolutions of various plasma parameters in the current ramp-up discharge, where an ice pellet is injected at 250 ms. The electron cyclotron emission (ECE) signal clearly shows the sawtooth oscillations having about 7 ms period, in the phase of high plasma current and high electron density after the pellet injection. Soft X-ray emission near the center shows m=1/n=1 oscillations about 10 ms before the ice pellet injection, and then shows clear sawtooth oscillations such as ECE signals.

Figure 4 shows measured Hα motional Stark spectra of the full energy beam emission at the radial position of R=97 cm. Although each motional Stark component is not well separated due to relatively large Doppler broadening of the line caused by a finite beam-divergence, the σ component of the full energy beam emission is comparatively well separated from the half energy beam emission and the π component manifolds, as seen from Fig. 4 (a). Figure 4 (b) shows the spectra of the full energy beam emission obtained from ±45° polarizers. The pitch angle is derived using central intensity of the σ component, while the spectra of the σ and π components from the 0° and 90° polarizers are utilized to monitor the intensity integration region. The pitch angle of internal magnetic field has been derived from the analysis of MSE spectra described in Subsection 2.2.

Figure 5 (a) shows the pitch angle as a function of the minor radius r (=R-Rax; Rax is the major radius of the magnetic axis) in the mid-plane, before(t=190 ms) and after (t=230 ms) the plasma current ramp up and after the ice pellet injection(t=270 ms), respectively (as seen from Fig.3). Note that because of the time resolution of our system, for instance, the profile at 190 ms means the profile averaged from 180 ms to 200 ms and the others also do. It is clear that the slope of the pitch angle at the plasma center become steeper with time. The poloidal magnetic field is derived from the pitch angle as $B_p = B_t \tan\alpha_p$, since the toroidal magnetic field is known beforehand. Figure 5 (b) shows the radial profiles of the poloidal magnetic field. For the JIPP T-IIU plasma having low beta and a circular plasma cross-section, the safety factor is straightforwardly estimated from the poloidal field as in Fig.5 (c). In particular, the safety factor at the plasma center q(0) is obtained from the slope of the pitch angle at the magnetic axis as,

$$q(0) = \frac{1}{R_{ax}\, d \tan \alpha_p / dr|_{r=0}},$$

In Fig.6 we show the time evolution of q(0) estimated by this equation together with the safety factor at the plasma surface q(a). Figure 6 also shows time evolution calculated from a magnetic diffusion equation based on neoclassical resistivity using experimentally obtained electron temperature and density profiles so that the calculated loop voltage and size of sawtooth inversion radius should agree with the experimental data[1]. Since poloidal beta value in this plasma is not significant ($\beta_p \leq 1$) and plasma collisionality is in the lower edge of plateau regime or higher edge of the banana one, the bootstrap current effect can be neglected . The q(0) measured with the MSE polarimetry agrees well with the calculated one based on the neoclassical resistivity, where uniform Zeff-profile gives good agreement in the size of sawtooth inversion radii. The value of q(0) is about 1.7 just before the current ramp-up and decreases during the ramp-up toward about unity around $t \approx 230$ -240 ms when m=1/n=1 oscillations appear on soft X-ray signal, as shown in Fig.3(b). Finally, the q(0) value reaches about 0.7 in the phase with the sawtooth oscillations.

The offset of the measured pitch angle is crucial to determine the poloidal magnetic field. In our arrangement, the offset may mainly be caused by the accuracy in a geometrical alignment of the polarizers. The offset is considered to be less than 0.5°, which is the maximum tilt angle of a flange of the port. We have assumed the offset to be 0.3°

throughout the discharge. In this discharge the major radius of the plasma is fluctuated by NBI heating between 88 cm and 92 cm. With this assumed offset value, the poloidal magnetic field obtained by the MSE polarimetry agrees with the values in the region of r/a=0.6-0.7 independently obtained by the Zeeman polarimeter[12], within experimental error bars. The position of magnetic axis estimated by the MSE polarimetry is also consistent with magnetic probe measurement. However, the size of the q=1 surface at t=270 ms is fairly large (~ 9 cm), compared with that estimated from ECE data (~ 5 cm). This discrepancy can be interpreted by the fairly large spatial resolution of about 4cm to 6 cm in the interested radial location, as described in subsection **2.1**.

§ 4. Discussion

The multichannel (i.e., 15 channels) MSE polarimetric measurement has revealed that a monotonical q-profile with q(0)~1.7 just before the rapid current ramp-up evolves to an almost similar profile shape during the current ramp-up, although the profile in the core plasma region tends to become flat. This time evolution of q-profile during the current ramp-up may be caused by relatively low electron temperature (Teo~1.5 keV), small minor radius ($a \leq 23$ cm) and low auxiliary heating power level ($P_{NBI} \leq 0.5$ MW). Moreover, in JIPP T-IIU, ice pellet injection usually enhances sawtooth activity instead of realization of magnetic shear reversal as observed in large tokamaks [2,5].

As mentioned above, the value q(0) obtained by this MSE polarimetry decreases monotonically from ~1.7 to ~1 just before the appearance of sawtooth oscillations. The significance of this measurement is that the q(0) value is decreased down to 0.7-0.8 during the sawtoothing phase in the ice-pellet-fueled high density plasma heated by neutral beam injection. The q-profile is considerably flat within q=1 surface. The time resolution is 20 ms, while the period of the sawtooth is about 7 ms as seen from Fig.3. Therefore, the q(0) value is averaged over about three sawtooth periods. If the time evolution of q(0) is assumed to be the following functional form during a sawtooth period of T as,

$$q(0)(t)=q(0)max-[q(0)max-q(0)min]\cdot[1-\exp(-t/\tau)]/[1-\exp(-T/\tau)],$$

the q(0) averaged over the period T is $\langle q(0)\rangle \approx [q(0)max+q(0)min]/2$ in the case of $T \ll \tau$, and $\langle q(0)\rangle \approx q(0)_{min}$ for $T \gg \tau$. If $q(0)_{max} = 1$ is assumed, for both cases the expected minimum value of q(0) is decreased well below unity , which cannot be explained by the Kadomtsev's complete reconnection model where q(0) should be near unity [20]. Our results suggest that a partial reconnection takes place at the sawtooth crash instead of the complete reconnection. In the previous JIPP T-IIU experiment, this possibility was discussed through a study of fast plasma cooling induced by ice pellet injection[21]. The evidence of q(0) well below unity is similar to the results observed on various discharge conditions of some tokamaks TEXTOR[9, 22], JET[23, 24], PBX-M[15], MTX[25], Tokapole II[26] and TEXT[27], but is in a marked contrast to the results from ASDEX[10], TCA[13], TEXT[28, 29], and DIII-D[30].

§ 5. Summary

Time evolution of the safety factor profile in the current ramp-up plasma has been successfully obtained with a 15-channel MSE polarimeter in JIPP T-IIU, employing a newly developed spectral analysis method where only σ-components are analyzed to avoid difficulty due to asymmetry of π-component. The newly developed two-polarizer method is demonstrated to be suitable for analyzing the MSE data obtained by a heating neutral beam with fairly large divergence (> 1°). In the current ramp-up discharge, q-profile evolves during the current ramp-up, keeping almost similar monotonical profile, instead of realizing a non-monotonical one. A fairly low q(0) (=0.7-0.8) is achieved during the sawtoothing phase, which obviously contradicts with the Kadomtev's complete reconnection sawtooth-model.

Acknowledgment

One of authors (J. Xu) would like to acknowledge Prof. M. Fujiwara, Prof. T. Kuroda and Prof. A. Iiyoshi for their continuous encouragement, and Dr. A. Fujisawa for some beneficial discussions.

References

[1] K.Toi, S. Itoh, K. Kadota, K. Kawahata, N. Noda et al., Nucl. Fusion **19** (1979) 1643.

[2] K.Toi, K. Kawahata, S. Morita, T. Watari, R. Kumazawa et al., Phys. Rev. Lett. **64** (1990) 1895.

[3] M.C. Zarnstorff, C.W. Barnes, P.C. Efthimion, G.W. Hammett, W. Horton et al., in Plasma Physics and Controlled Nuclear Fusion Research 1990 (Proc. 13th Int. Conf., Washington, D.C., 1990), Vol.1, IAEA, Vienna (1991)109.

[4] M.E. Mauel, G.A. Navratil, S.A. Sabbagh, S.H. Batha, M.G. Bell et al., in Plasma Physics and Controlled Nuclear Fusion Research 1992 (Proc. 14th Int. Conf., Würtzburg, 1992), Vol.1, IAEA, Vienna (1993)205.

[5] Tubbing, B et al., Nucl. Fusion **31** (1991) 839.

[6] Hugon, M et al., Nucl. Fusion **32** (1992) 33.

[7] DIII-D Team, in Plasma Physics and Controlled Nuclear Fusion Research 1994 (Proc. 15th Int. Conf., Seville, 1994), Vol.1, IAEA, Vienna (1995)83.

[8] Garbet, X. et al, in Plasma Physics and Controlled Nuclear Fusion Research 1994 (Proc. 15th Int. Conf., Seville, 1994), Vol.1, IAEA, Vienna (1995) 341.

[9]. H. Soltwisch, Rev. Sci. Instrum. **57** (1986) 1939.

[10]. K. McCormick et al., Phys. Rev. Lett. **58** (1987) 491.

[11]. D. Wroblewski, L.K.Huang, and H.W. Moos, Rev. Sci. Instrum. **59** (1988) 2341.

[12] H. Kuramoto, N. Hiraki, S. Moriyama, K. Toi, K. Sato et al., "Measurement of the Poloidal Magnetic Field Profile with High Time Resolution Zeeman Polarimeter in the JIPP T-IIU Tokamak", to be published in Fusion Engineering and Designs (1996).

[13] H. Weisen, G. Borg, B. Joye, A.J. Knight, J.B. Lister, Phys. Rev. Lett. **62** (1989) 434.

[14]. F. Alladio and M. Martone, Phys. Lett. A60, 39(1977)

[15]. F. M. Levinton, R. J. Fonck, G. M. Gammel, R. Kaita, H. W. Kugel, E. T. Powell and D. W. Roberts, Phys. Rev. Lett. **63**, 2060(1989).

[16]. D. Wroblewski, K.H.Burrell, L.L.Lao, P.Politzer and W.P.West, Rev. Sci. Instrum. **63** (1992) 5140.

[17]. W Mandle, R.C. Wolf, M. Von Hellermann and H P Summers, Plasma Phys. Control. Fusion 35(1993) 1373-1397.

[18] K. Toi, Y. Hamada, K. Kawahata, T. Watari, A. Ando et al., in Plasma Physics and Controlled Nuclear Fusion Research 1990 (Proc. 13th Int. Conf., Washington, D.C., 1990), Vol.1, IAEA, Vienna (1991).301.

[19]. E.U. Condon and G.H.shortley, *The Theory of Atomic Spectra* (Cambridge University, Cambridge, 1963)

[20] B.B. Kadomtev, Sov. J. Plasma Phys. **1** (1975) 389.

[21] M. Sakamoto, K.N. Sato, Y. Ogawa, K. Kawahata, S. Hirokura et al., Plasma Phys. Controlled Fusion **33** (1991) 583.

[22] B. Ph. van Milligen, H. Soltwisch, N.J. Lopes Cardozo, Nucl. Fusion **31** (1991) 309.

[23] J. O'Rourke, Plasma Phys. Controlled Fusion **33** (1991) 289.

[24] R.C. Wolf, J. O'Rourke, A.W. Edwards, M. von Hellermann, Nucl. Fusion **33** (1993) 663.

[25] B.W. Rice, Rev. Sci. Instrum. **63** (1992) 5002.

[26] T.H. Osborne, R.N. Dexter, S.C. Prager, Phys. Rev. Lett. **49** (1982) 734.

[27] W. P. West, D.M. Thomas, J.S. de Grassie, S.B. Zheng, Phys. Rev. Lett. **58** (1987) 2758.

[28] D. Wróblewski, L.K. Huang, H.W. Moos, P.E. Phillips, Phys. Rev. Lett. **61** (1988) 1724.

[29] K.H. Huang, M. Finkenthal, D. Wróblewski, H.W. Moos, W.P. West et al., Phys. Fluids **B2** (1990) 809.

[30] D. Wróblewski, R.T. Snider, Phys. Rev. Lett. **71** (1993) 859.

Figure Captions

Fig. 1 A schematic of the experimental arrangement of the MSE polarimeter system in the JIPP T-IIU tokamak.

Fig. 2 A schematic of the pattern of the σ component transmission of the beam emission along the viewing line in the mid-plane.

Fig. 3 Time evolutions of plasma current(I_p), line-averaged electron density(n_e), $H\alpha/D\alpha$-light($H\alpha/D\alpha$), electron temperatures at $r/a \approx 0$ and 0.3 obtained from ECE (T_e), and soft X-ray near the plasma center(I_{sxo}) in the current ramp-up plasma where the MSE polarimetry is carried out. A neutral hydrogen beam with 30 keV energy is injected into the plasma, where the heating power is 0.5 MW and the toroidal field B_t =3 T. The soft X-ray signal is modulated by m=1/n=1 oscillations from t $\approx$ 240 ms, and then exhibits clear sawtooth oscillations just after the pellet injection (at t=250 ms) as well as ECE signals.

Fig. 4 Measured motional Stark spectra of the hydrogen beam emission experimentally obtained from 0°, 45°, 90° and 135° tilted polarizers. (a) σ and π manifolds from 0° and 90° tilted polarizers and (b) the spectra of the full energy beam emission from 45° and 135° tilted polarizers.

Fig. 5 Radial profiles of the pitch angle of the internal magnetic field(a), the poloidal magnetic field (b) and the safety factor (c), before(t=190 ms), after the plasma current ramp-up (t=230 ms) and after the ice pellet injection (t=270 ms)when the sawtooth oscillations are excited. Magnetic axis position R_{ax} is 93, 91 and 90 cm at 190 ms, 230 ms and 270 ms, respectively.

Fig. 6 Time evolution of the q(0) derived from the MSE polarimetry(solid circles) and q(0) calculated from the magnetic diffusion equation based on experimentally obtained radial profiles of electron temperature and density and neoclassical resistivity(open circles). The safety factor at the plasma surface derived from magnetic probes is also shown.

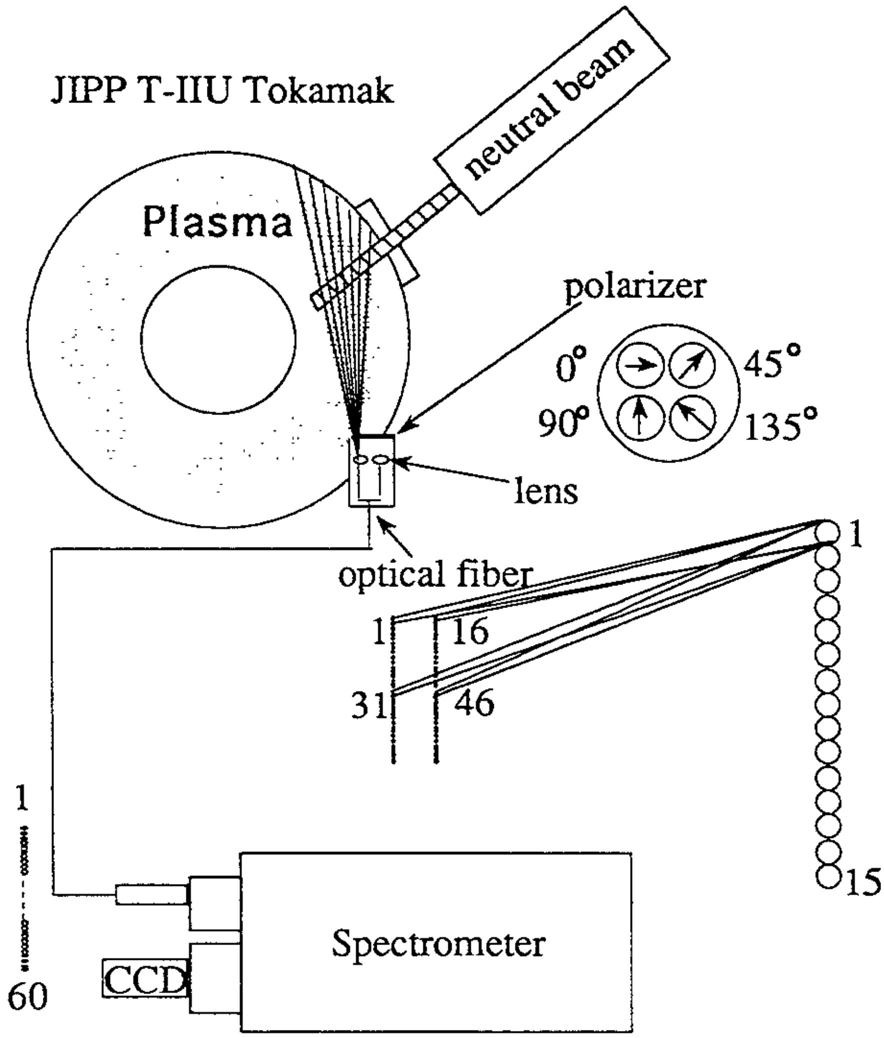

Fig.1 J. Xu et al.

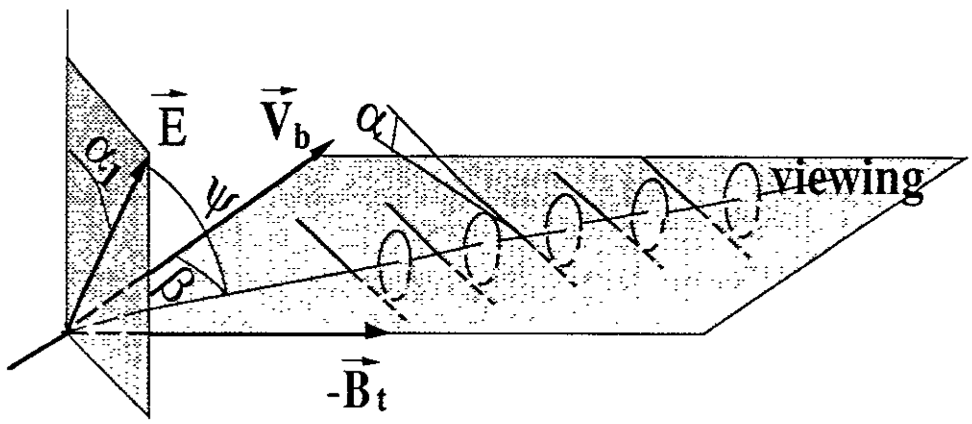

Fig.2 J. Xu et al.

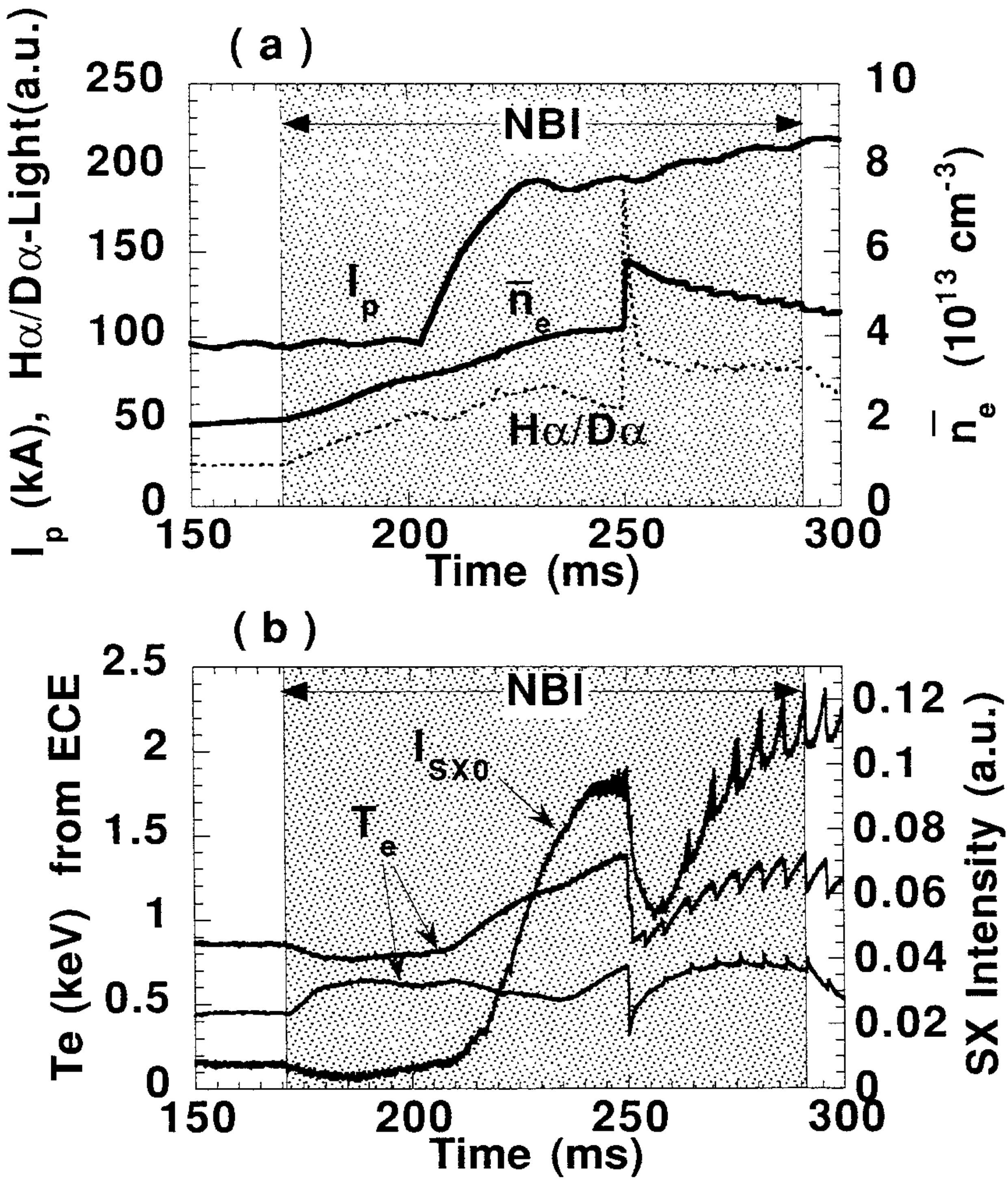

Fig.3 J. Xu et al.

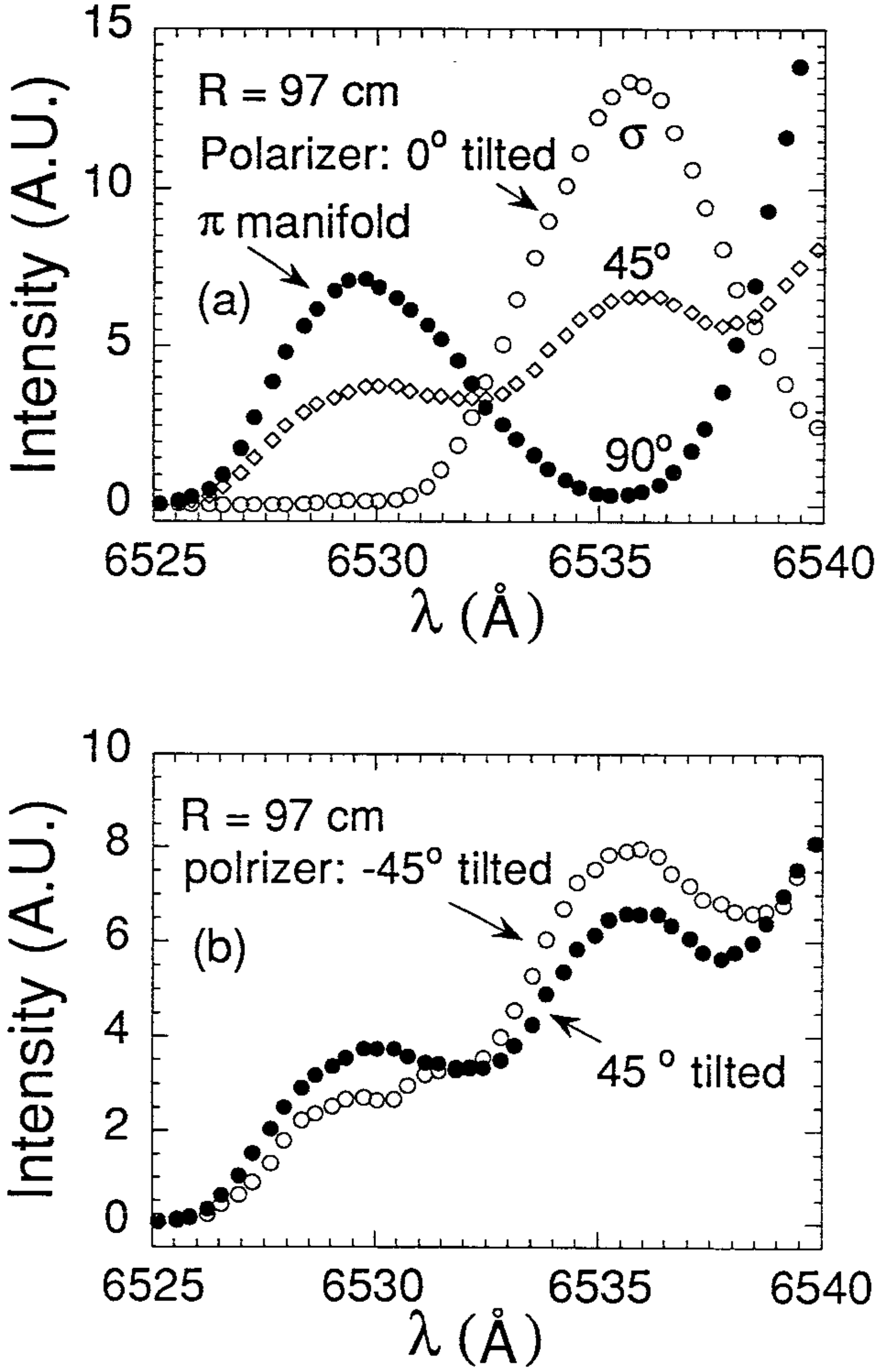

Fig.4 J. Xu et al.

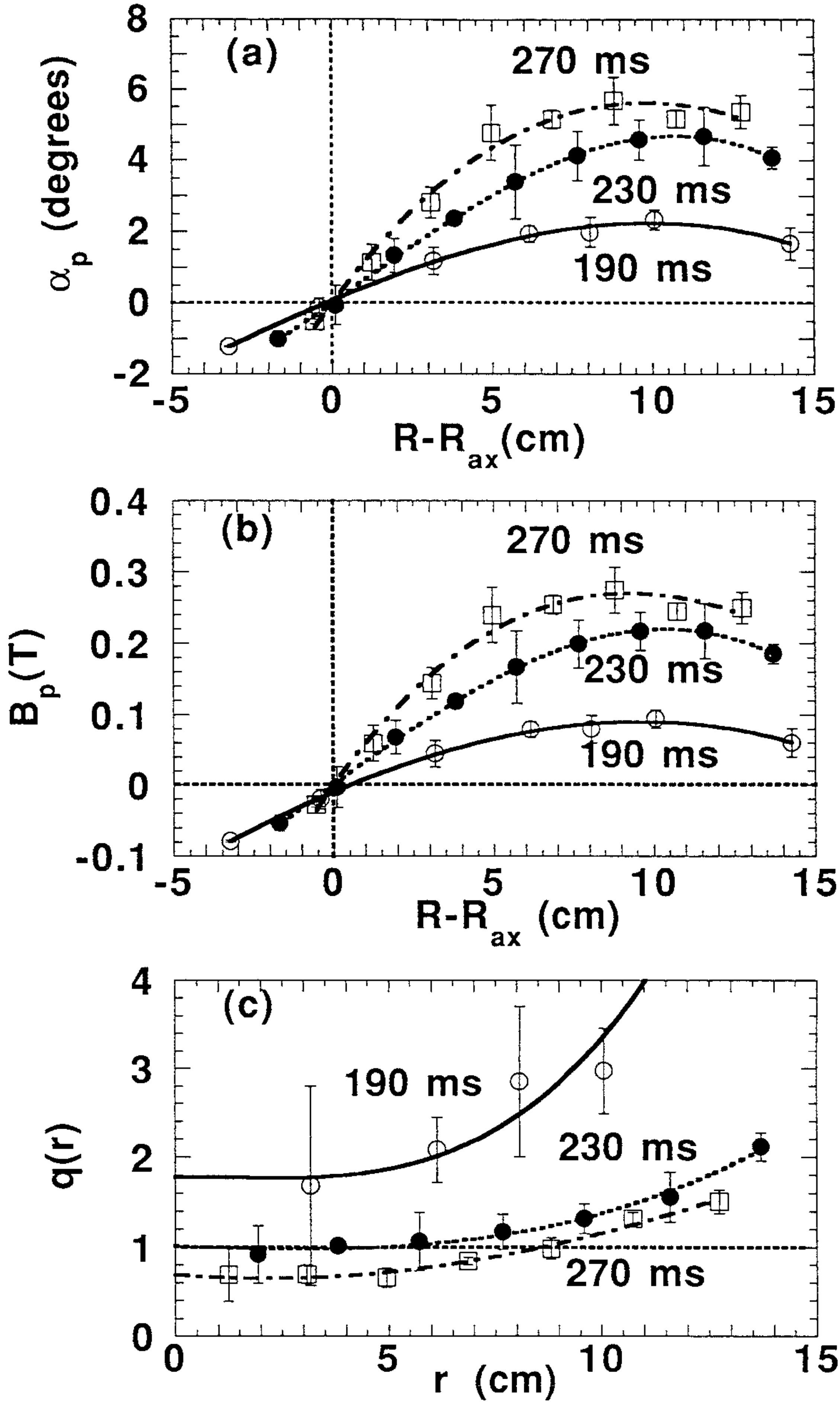

Fig.5 J. Xu et al.

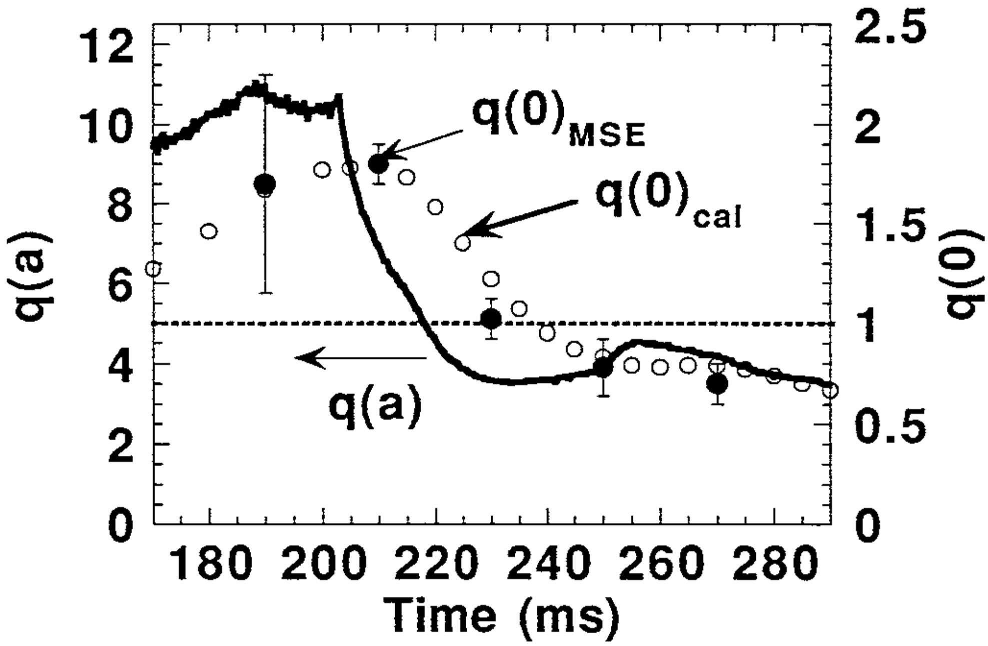

Fig.6 J. Xu et al.

Recent Issues of NIFS Series

NIFS-372 H. Miura,
Enstrophy Generation in a Shock-Dominated Turbulence; Sep. 1995

NIFS-373 M. Natsir, A. Sagara, K. Tsuzuki, B. Tsuchiya, Y. Hasegawa, O. Motojima,
Control of Discharge Conditions to Reduce Hydrogen Content in Low Z Films Produced with DC Glow; Sep. 1995

NIFS-374 K. Tsuzuki, M. Natsir, N. Inoue, A. Sagara, N. Noda, O. Motojima, T. Mochizuki, I. Fujita, T. Hino and T. Yamashina,
Behavior of Hydrogen Atoms in Boron Films during H_2 *and He Glow Discharge and Thermal Desorption;* Sep. 1995

NIFS-375 U. Stroth, M. Murakami, R.A. Dory, H. Yamada, S. Okamura, F. Sano and T. Obiki,
Energy Confinement Scaling from the International Stellarator Database; Sep. 1995

NIFS-376 S. Bazdenkov, T. Sato, K. Watanabe and The Complexity Simulation Group,
Multi-Scale Semi-Ideal Magnetohydrodynamics of a Tokamak Plasma; Sep. 1995

NIFS-377 J. Uramoto,
Extraction of Negative Pionlike Particles from a H2 or D2 Gas Discharge Plasma in Magnetic Field; Sep. 1995

NIFS-378 K. Akaishi,
Theoretical Consideration for the Outgassing Characteristics of an Unbaked Vacuum System; Oct. 1995

NIFS-379 H. Shimazu, S. Machida and M. Tanaka,
Macro-Particle Simulation of Collisionless Parallel Shocks; Oct. 1995

NIFS-380 N. Kondo and Y. Kondoh,
Eigenfunction Spectrum Analysis for Self-organization in Dissipative Solitons; Oct. 1995

NIFS-381 Y. Kondoh, M. Yoshizawa, A. Nakano and T. Yabe,
Self-organization of Two-dimensional Incompressible Viscous Flow in a Friction-free Box; Oct. 1995

NIFS-382 Y.N. Nejoh and H. Sanuki,
The Effects of the Beam and Ion Temperatures on Ion-Acoustic Waves in an Electron Beam-Plasma System; Oct. 1995

NIFS-383 K. Ichiguchi, O. Motojima, K. Yamazaki, N. Nakajima and M. Okamoto
Flexibility of LHD Configuration with Multi-Layer Helical Coils;

Nov. 1995

NIFS-384 D. Biskamp, E. Schwarz and J.F. Drake,
Two-dimensional Electron Magnetohydrodynamic Turbulence; Nov. 1995

NIFS-385 H. Kitabata, T. Hayashi, T. Sato and Complexity Simulation Group,
Impulsive Nature in Collisional Driven Reconnection; Nov. 1995

NIFS-386 Y. Katoh, T. Muroga, A. Kohyama, R.E. Stoller, C. Namba and O. Motojima,
Rate Theory Modeling of Defect Evolution under Cascade Damage Conditions:The Influence of Vacancy-type Cascade Remnants and Application to the Defect Production Chracterization by Microstructural Analysis; Nov. 1995

NIFS-387 K. Araki, S. Yanase and J. Mizushima,
Symmetry Breaking by Differential Rotation and Saddle-node Bifurcation of the Thermal Convection in a Spherical Shell; Dec. 1995

NIFS-388 V.D. Pustovitov,
Control of Pfirsch-Schlüter Current by External Poloidal Magnetic Field in Conventional Stellarators: Dec. 1995

NIFS-389 K. Akaishi,
On the Outgassing Rate Versus Time Characteristics in the Pump-down of an Unbaked Vacuum System; Dec. 1995

NIFS-390 K.N. Sato, S. Murakami, N. Nakajima, K. Itoh,
Possibility of Simulation Experiments for Fast Particle Physics in Large Helical Device (LHD); Dec. 1995

NIFS-391 W.X.Wang, M. Okamoto, N. Nakajima, S. Murakami and N. Ohyabu,
A Monte Carlo Simulation Model for the Steady-State Plasma in the Scrape-off Layer; Dec. 1995

NIFS-392 Shao-ping Zhu, R. Horiuchi, T. Sato and The Complexity Simulation Group,
Self-organization Process of a Magnetohydrodynamic Plasma in the Presence of Thermal Conduction; Dec. 1995

NIFS-393 M. Ozaki, T. Sato, R. Horiuchi and the Complexity Simulation Group
Electromagnetic Instability and Anomalous Resistivity in a Magnetic Neutral Sheet; Dec. 1995

NIFS-394 K. Itoh, S.-I Itoh, M. Yagi and A. Fukuyama,
Subcritical Excitation of Plasma Turbulence; Jan. 1996

NIFS-395 H. Sugama and M. Okamoto, W. Horton and M. Wakatani,
Transport Processes and Entropy Production in Toroidal Plasmas with Gyrokinetic Eletromagnetic Turbulence; Jan. 1996

NIFS-396 T. Kato, T. Fujiwara and Y. Hanaoka,
X-ray Spectral Analysis of Yohkoh BCS Data on Sep. 6 1992 Flares - Blue Shift Component and Ion Abundances -; Feb. 1996

NIFS-397 H. Kuramoto, N. Hiraki, S. Moriyama, K. Toi, K. Sato, K. Narihara, A. Ejiri, T. Seki and JIPP T-IIU Group,
Measurement of the Poloidal Magnetic Field Profile with High Time Resolution Zeeman Polarimeter in the JIPP T-IIU Tokamak; Feb. 1996

NIFS-398 J.F. Wang, T. Amano, Y. Ogawa, N. Inoue,
Simulation of Burning Plasma Dynamics in ITER; Feb. 1996

NIFS-399 K. Itoh, S-I. Itoh, A. Fukuyama and M. Yagi,
Theory of Self-Sustained Turbulence in Confined Plasmas; Feb. 1996

NIFS-400 J. Uramoto,
A Detection Method of Negative Pionlike Particles from a H2 Gas Descharge Plasma; Feb. 1996

NIFS-401 K.Ida, J.Xu, K.N.Sato, H.Sakakita and JIPP TII-U group,
Fast Charge Exchange Spectroscopy Using a Fabry-Perot Spectrometer in the JIPP TII-U Tokamak; Feb. 1996

NIFS-402 T. Amano,
Passive Shut-Down of ITER Plasma by Be Evaporation; Feb. 1996

NIFS-403 K. Orito,
A New Variable Transformation Technique for the Nonlinear Drift Vortex; Feb. 1996

NIFS-404 T. Oike, K. Kitachi, S. Ohdachi, K. Toi, S. Sakakibara, S. Morita, T. Morisaki, H. Suzuki, S. Okamura, K. Matsuoka and CHS group; *Measurement of Magnetic Field Fluctuations near Plasma Edge with Movable Magnetic Probe Array in the CHS Heliotron/Torsatron*; Mar. 1996

NIFS-405 S.K. Guharay, K. Tsumori, M. Hamabe, Y. Takeiri, O. Kaneko, T. Kuroda,
Simple Emittance Measurement of H- Beams from a Large Plasma Source; Mar. 1996

NIFS-406 M. Tanaka and D. Biskamp,
Symmetry-Breaking due to Parallel Electron Motion and Resultant Scaling in Collisionless Magnetic Reconnection; Mar. 1996

NIFS-407 K. Kitachi, T. Oike, S. Ohdachi, K. Toi, R. Akiyama, A. Ejiri, Y. Hamada, H.Kuramoto, K. Narihara, T. Seki and JIPP T-IIU Group,
Measurement of Magnetic Field Fluctuations within Last Closed Flux Surface with Movable Magnetic Probe Array in the JIPP T-IIU Tokamak; Mar. 1996

NIFS-408 K. Hirose, S. Saito and Yoshi.H. Ichikawa
Structure of Period-2 Step-1 Accelerator Island in Area Preserving Maps; Mar. 1996

NIFS-409 G.Y.Yu, M. Okamoto, H. Sanuki, T. Amano,
Effect of Plasma Inertia on Vertical Displacement Instability in Tokamaks; Mar. 1996

NIFS-410 T. Yamagishi,
Solution of Initial Value Problem of Gyro-Kinetic Equation; Mar. 1996

NIFS-411 K. Ida and N. Nakajima,
Comparison of Parallel Viscosity with Neoclassical Theory; Apr. 1996

NIFS-412 T. Ohkawa and H. Ohkawa,
Cuspher, A Combined Confinement System; Apr. 1996

NIFS-413 Y. Nomura, Y.H. Ichikawa and A.T. Filippov,
Stochasticity in the Josephson Map; Apr. 1996

NIFS-414 J. Uramoto,
Production Mechanism of Negative Pionlike Particles in H_2 *Gas Discharge Plasma*; Apr. 1996

NIFS-415 A. Fujisawa, H. Iguchi, S. Lee, T.P. Crowley, Y. Hamada, S. Hidekuma, M. Kojima,
Active Trajectory Control for a Heavy Ion Beam Probe on the Compact Helical System; May 1996

NIFS-416 M. Iwase, K. Ohkubo, S. Kubo and H. Idei
Band Rejection Filter for Measurement of Electron Cyclotron Emission during Electron Cyclotron Heating; May 1996

NIFS-417 T. Yabe, H. Daido,T. Aoki, E. Matsunaga and K. Arisawa,
Anomalous Crater Formation in Pulsed-Laser-Illuminated Aluminum Slab and Debris Distribution; May 1996

NIFS-418 J. Uramoto,
Extraction of K^- *Mesonlike Particles from a* D_2 *Gas Discharge Plasma in Magnetic Field;* May 1996

NIFS-419 J. Xu, K. Toi, H. Kuramoto, A. Nishizawa, J. Fujita, A. Ejiri, K. Narihara, T. Seki, H. Sakakita, K. Kawahata, K. Ida, K. Adachi, R. Akiyama, Y. Hamada, S. Hirokura, Y. Kawasumi, M. Kojima, I. Nomura, S. Ohdachi, K.N. Sato
Measurement of Internal Magnetic Field with Motional Stark Polarimetry in Current Ramp-Up Experiments of JIPP T-IIU; June 1996